Colloid Polym Sci (2002) 280: 1062–1066
DOI 10.1007/s00396-002-0698-8

ORIGINAL CONTRIBUTION

Y.H. Cho
M.S. Cho
H.J. Choi
M.S. Jhon

Electrorheological characterization of polyaniline-coated poly(methyl methacrylate) suspensions

Received: 24 October 2001
Accepted: 19 March 2002

Y.H. Cho · M.S. Cho · H.J. Choi (✉)
Department of Polymer Science
and Engineering, Inha University,
Incheon, 402-751, Korea
E-mail: hjchoi@inha.ac.kr
Tel.: +82 32 860 7486
Fax: +82 32 865 5178

M.S. Jhon
Department of Chemical Engineering,
Carnegie Mellon University, Pittsburgh,
PA 15213-3890, USA

Abstract Surface-conductive particles consisting of a poly(methyl methacrylate) (PMMA) core and a polyaniline (PA)-coated shell were synthesized and adopted as suspended particles for electrorheological (ER) fluids. The PA–PMMA composite particles synthesized were monodisperse and spherical in shape. The PA–PMMA suspensions in silicone oil showed typical ER characteristics under an applied electric field. The PA–PMMA composite particles possess a higher dielectric constant and conductivity than the pure PA particle, within an acceptable conductivity range for ER fluids, but the PA-based ER fluid showed larger shear-stress enhancement than the PA–PMMA-based systems. This phenomena can be explained by the interfacial polarizability of PA-based ER fluids, which is the difference between the ER fluid's dielectric constant and loss factor – this polarizability was higher than that of PA–PMMA-based ER fluids, as shown by the dielectric spectrum of each fluid. The insulating PMMA core suppressed the interfacial polarization in ER fluids, resulting in reduced interaction among particles under an imposed electric field.

Keywords Electrorheological fluid · Polyaniline · Microsphere · Polarizability · Suspension

Introduction

Electrorheological (ER) fluids are suspensions of dielectric (or polarizable) particles in a nonconducting liquid [1, 2, 3, 4] and exhibit drastic changes in their rheological properties, which include a large increase in apparent viscosity and the formation of reversible suspension microstructures under an applied electric field [5, 6]. Shear-stress models have been introduced to describe the ER phenomena [7, 8]. The original model, the "polarization model," attributed the attractive force among particles to Maxwell–Wagner interfacial polarization [9, 10] and employed the point-dipole approximation, indicating that the suspended particles are polarized owing to a dielectric mismatch between the particles and the suspending fluid under an applied electric field, and then the interaction among the polarized particles causes them to arrange into strings along the direction of the electric field. On the other hand, as the gap between the conducting particles in the fluid decreases, the fluid's electric response becomes nonlinear via electrical breakdown under high electric field strengths. This nonlinear conductivity model for ER fluids is a recent one [1, 11]. Clearly, the ER performance depends on the electrical properties of the suspended particles [12].

ER characteristics, such as the quickly reversible change and tunable viscosity via an imposed electric field, find practical applications in electromechanical devices, for example, including engine mounts, shock absorbers, clutches, ER valves, robotic arms, and other various control systems [11, 13]. Nonetheless, ER devices have not been fully commercialized, even though they have many potential applications in industry. The major stumbling blocks are a lack of a reliable, cost-effective synthesis techniques, and a lack of understanding in the underlying ER molecular mechanisms. During theoretical development, the suspended particles in ER fluids are assumed to be monodisperse and spherical; however, the particles used in ER fluids are generally polydisperse and possess an irregular shape [14, 15]. These factors are one of the most critical yet difficult parameters in constructing a theoretical model. Several attempts have been made to use ideal, well-characterized particles, such as TiO_2-coated Ni [16], polyaniline (PA)-coated silica [17], microencapsulated PA [18], poly(methyl methacrylate) (PMMA) with a double-layered shell [19], and PA–clay nanocomposite [20, 21]. Various conducting polymer-coated latex particles (including PA-coated polystyrene particles [22] and polypyrrole-coated polystyrene particles [23]) have also been investigated [24]. The ER properties for these particles have not yet been carefully investigated.

In this study, we introduce a core–shell system using a monodisperse PMMA core and a PA shell with a monodisperse and spherical particle as potential candidates for a model of the dispersed phase of an ER fluid. The ER properties of these particles were examined and compared to an ER fluid using only the PA particle.

Method

The monodisperse, spherical PMMA particles were synthesized via a dispersion polymerization method [25], which is one of the preferred methods for preparing monodisperse polymer particles. The distilled methyl methacrylate monomer (Aldrich, USA) and a radical initiator (azoisobutyronitrile) (Aldrich, USA) were dissolved at 10 and 0.1 wt%, respectively, in methanol containing 4 wt% of poly(vinyl pyrrolidone) (ISP, USA) as a stabilizer at 25 °C. After purging with nitrogen to remove oxygen, the reaction mixture was heated to 55 °C and then kept for 24 h. The synthesized monodisperse particles of 2 μm were washed with methanol and then dispersed in water prior to the PA polymerization.

The PA–PMMA microspheres synthesized were then prepared via a protocol established by Barthet et al. [22]. The PMMA particles were first dispersed at 5 wt% in a 0.0095 M sodium dodecyl sulfate (SDS) aqueous solution and kept under mild stirring to allow the SDS to contact and adsorb onto the PMMA surfaces. Aniline (4 and 20 g per 100 g PMMA) was added to this suspension to produce PA–PMMA4 and PA–PMMA20. A small amount of hydroquinone was also added to this reaction system to minimize the polymerization of aniline in the water phase. Finally, it was acidified to a pH of 0.7 using HCl, and then a solution of ammonium peroxysulfate (APS) was put in the reaction system as an initiator [26, 27, 28]. The molar ratio of APS to aniline was 1.25. The polymerization was continued for 24 h at 25 °C. The PA–PMMA composite particles were washed and their conductivities were controlled by the same procedure as PA [29] in the range between 10^{-9} and 10^{-10} Scm^{-1}, which is the desirable range for particles used in ER fluids. After adjusting the conductivity, the products were dried in a vacuum oven at 25 °C. ER fluids of 10 vol% were prepared by dispersing dried PA–PMMA particles in silicone oil.

In order to compare the ER performances, a PA homopolymer particle was prepared using HCl dopant following the method previously reported [30, 31]. It was also washed and dedoped after synthesis. The dried PA particle was then dispersed in the silicone oil.

Scanning electron microscope (SEM) photographs of the monodisperse PMMA and PA–PMMA particles are shown in Fig. 1. Although the coated surface of the PA–PMMA particles with PA is not perfectly smooth, the monodispersity of the particles is maintained.

The conductivity and dielectric constant of pressed disk-type PA–PMMA particles were measured via the two-probe method using a picoammeter with an internal voltage source (487, Keithley, USA) and an impedance analyzer (4284A, HP, USA), respectively [32]. The thickness of the PA-coated layer was measured via thermogravimetric analysis (TGA) at 400 °C. Note that the PMMA decomposed almost entirely at this temperature. The physical properties of PA–PMMAs and PA are summarized in Table 1.

Both the electric conductivity and the dielectric constant increase with PA shell thickness. To quantify the amount of coated PA, we defined PA–PMMA*X* as *X* g aniline monomer per 100 g PMMA during the synthesis. The actual amount of aniline was measured via TGA, as given in Table 1.

The ER properties of the PA–PMMA-based and PA-based ER fluids were examined via a rotational rheometer (MC120, Paar-Physica, Germany) equipped with a high direct current voltage generator and concentric cylinder-type measuring unit by shear-stress and shear-rate control techniques. Specifically, the flow curve was measured via a controlled-shear-rate mode in the shear-rate

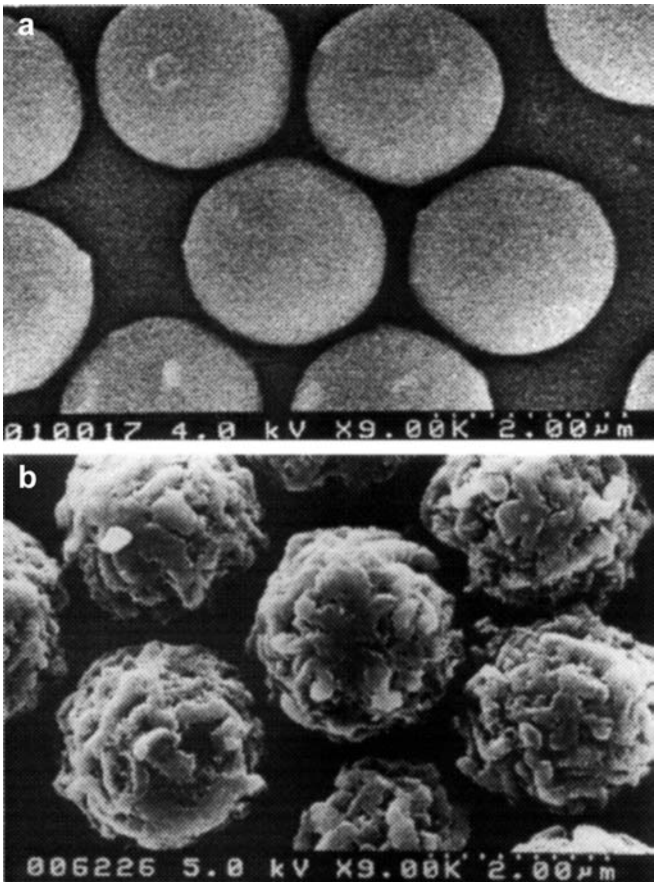

Fig. 1. Scanning electron microscopy photos of (**a**) poly(methyl methacrylate) (PMMA) seed particles and (**b**) polyaniline (*PA*)–PMMA20 particles

Table 1. Polyaniline (*PA*) layer thicknesses and electrical properties of PA–poly(methyl methacrylate) (*PMMA*) and PA

Sample code	PA layer thickness (nm)[a]	Weight percent of PA[b]	Conductivity (S/cm)	Dielectric constant[c]
PA–PMMA4	11	3.6	3.2×10^{-10}	6.82
PA–PMMA20	52	17.7	8.0×10^{-9}	15.75
PA[d]		100	1.0×10^{-11}	6.99

[a] Assuming that the PA layer has uniform thickness
[b] Measured via thermogravimetric analysis
[c] Measured at 1 kHz
[d] Synthesized under the reaction conditions given in Ref. [22]

range from 0.01 to 1,000 s^{-1} with a stepwise increment (each step takes approximately 6 s). Dielectric spectra of the ER fluids were also measured from 20 to 10^6 Hz using the impedance analyzer with a liquid fixture (16452A, HP, USA) at 25 °C [32].

Results and discussion

The flow curves of the ER fluids with PA–PMMA20 and PA particles dispersed in silicone oil for 10 vol% at various electric field strengths are shown in Fig. 2. These ER fluids generally show the flow properties of a Bingham fluid with yield stress (τ_0) [5, 15].

$$\tau = \tau_0 + \eta\dot{\gamma} \quad (\tau > \tau_0) \tag{1}$$

Here, τ is a shear stress, τ_0 is a yield stress, η is a shear viscosity after the yield point, and $\dot{\gamma} \equiv d\gamma/dt$ is a shear rate related to a strain (γ).

τ increases with the electric field strength for broad ranges of $\dot{\gamma}$; however, τ slightly decreases as $\dot{\gamma}$ increases up to a critical shear rate, $\dot{\gamma}_{\mathrm{crit}}$ (which is a typical trend of ER fluids [33, 34]). Here, $\dot{\gamma}_{\mathrm{crit}}$is a transition point to the Newtonian-flow region where the shear stress increases linearly with shear rate [30, 35]. Recently See et al. [36] reported that the decrease in τ with increasing $\dot{\gamma}$ occurs only under direct current electric fields. The shear-stress enhancement is due to the fibril structure of the particles formed by an applied electric field. When the shear deformation is applied, the fibrils begin to break apart and reform repeatedly, depending on the magnitude of the applied shear and the particle–particle interaction in the fibrils. As $\dot{\gamma}$ increases, the destruction rate of the fibrils becomes faster than the reformation rate. This is the reason why τ decreases for $\dot{\gamma} < \dot{\gamma}_{\mathrm{crit}}$. For $\dot{\gamma} > \dot{\gamma}_{\mathrm{crit}}$, the hydrodynamic interaction among the particles or clusters becomes dominant over the re-formation of the fibril structures, so the ER fluids exhibit Newtonian-flow behavior, as found in dilute suspension systems.

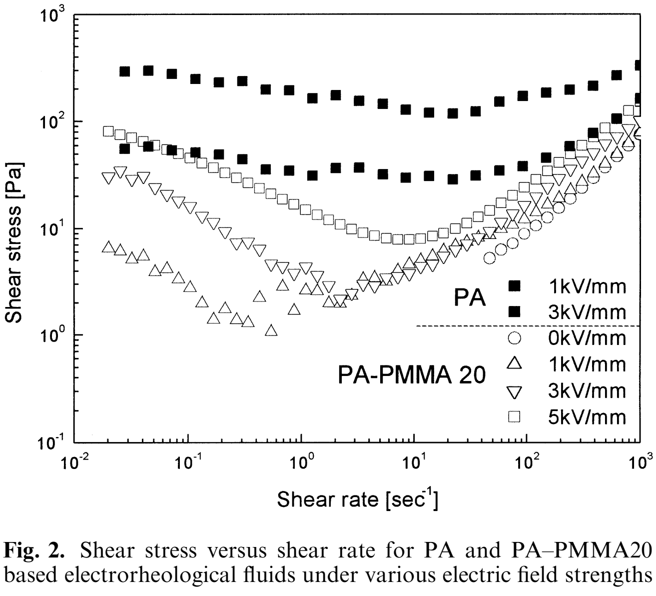

Fig. 2. Shear stress versus shear rate for PA and PA–PMMA20 based electrorheological fluids under various electric field strengths

The PA–PMMA4-based ER fluids have flow characteristics similar to PA–PMMA20-based ER fluids under imposed electric fields; however, the PA-based ER fluid shows a drastically different flow response and its stress enhancement is larger than that of the PA–PMMA series when compared to the electric field strength of 3 kVmm^{-1}. Considering the electrical properties of the PA and PA–PMMA particles (Table 1) in the light of previously reported results [27, 29, 37], the PA–PMMA systems are expected to show a better ER performance. However, the result in Fig. 2 does not indicate such an improvement. We speculate that the cause is as follows.

It has been suggested that interfacial polarization is an important factor in determining ER performance [10, 38]. The Cole–Cole plots of ER fluids shown in Fig. 3 support this explanation. The interfacial polarization of suspensions is a typical property of ER fluids with a polarizable dispersed phase and an insulating medium. The interfacial polarization induced by an external alternating current electric field is delayed as the frequency (ω) increases. ϵ' decreases from ϵ_0 $\left(\varepsilon_0 = \lim\limits_{\omega\to 0} \varepsilon'\right)$and ϵ' has a peak in the dielectric spectrum [39]. The lines in Fig. 3 are obtained by the fitting data to the Cole–Cole formula [40]:

$$\varepsilon^* = \varepsilon' + i\varepsilon'' = \varepsilon_\infty + \frac{\varepsilon_0 - \varepsilon_\infty}{1 + (i\omega\lambda)^{1-\alpha}} \quad (0 \le \alpha < 1), \tag{2}$$

where the exponent (1–α) characterizes the broadness of the relaxation time distribution and $i = \sqrt{-1}$. When $\alpha = 0$, Eq. (2) reduces to Debye's well-known single relaxation time model. Here, λ is the characteristic time.

The parameters that appear in Eq. (2) are summarized in Table 2. Although ϵ_0 is not directly shown in the experimental results, it can be determined from the second intercept on the ϵ'-axis by fitting the data to the Cole–Cole arc. $\Delta\epsilon \equiv (\epsilon_0 – \epsilon_\infty)$ is the achievable polarizability in an ER fluid. λ is related to the yield stress and

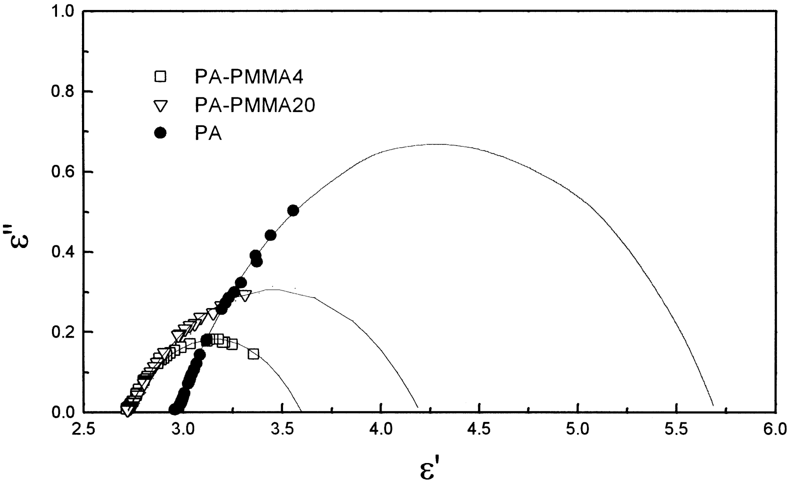

Fig. 3. Cole–Cole arc of electrorheological fluids. The *lines* are obtained from Eq. (2)

Table 2. Parameters in Eq. (2) obtained via the dielectric spectra of electrotheological (*ER*) fluids

ER fluids	ϵ_0	ϵ_∞	$\Delta\epsilon \equiv \epsilon_0 - \epsilon_\infty$	λ (s)	α
PA–PMMA4	3.6	2.72	0.88	0.002	0.50
PA–PMMA20	4.2	2.72	1.48	0.020	0.50
PA	5.7	2.96	2.74	0.040	0.41

the stress enhancement of ER fluids under an applied electric field. As λ becomes smaller within an adequate range, the stress enhancement is achieved [37]. In addition to λ, Hao [38] also suggested the role of tan δ ($=\epsilon'/\epsilon''$) of the particle in determining ER properties. However, the dependence of $\Delta\epsilon$ on the ER properties was not examined carefully in any previous report.

Even though the PA particle has the lowest dielectric constant among the particles studied here, ϵ_0 and $\Delta\epsilon$ of the PA suspension are higher than for the others, indicating that the interfacial polarization of the PA-based ER fluid is larger than PA–PMMA-based ER fluids. λ is no longer related to the ER performance in this series. It is understood that the insulating PMMA core counteracts the interfacial polarization of PA–PMMA-based ER fluids, and therefore lessens the electrically induced interactions among the particles. The PA suspension exhibits its best ER performance despite its inferior electrical properties owing to the superior $\Delta\epsilon$ of the PA–PMMA suspensions, suggesting that $\Delta\epsilon$ is an important factor in determining the ER properties.

Conclusion

Microspheres with a semiconductive PA shell and an insulating PMMA core were used for the dispersed phase of ER fluids and were then characterized using SEM, TGA, and impedance analysis. The PA–PMMA-based suspensions showed typical ER properties under an applied electric field, suggesting that the shear stress increases with the electric field strength for broad ranges of shear rate.

Furthermore, the characteristics of the ER fluids were explained by assuming the insulating PMMA core interfered with the interfacial polarization of the PA–PMMA suspension under an applied electric field, and this was subsequently confirmed by analysis of the dielectric spectra for the ER suspensions.

Acknowledgements This study was supported by research grants from the 2001 National Research Laboratory program, Korea.

References

1. Gonon P, Foulc JN, Atten P (2001) Int J Mod Phys B 15:704–713
2. Rejon L, Castaneda-Aranda I, Manero O (2001) Colloids Surf A 182:93–107
3. See H (1999) Korea-Aust Rheol J 11:169–195
4. Choi HJ, Cho MS, Kim JW, Kim CA, Jhon MS (2001) Appl Phys Lett 78:3806–3808
5. Parthasarathy M, Klingenberg DJ (1996) Mater Sci Eng R17:57–103
6. Choi HJ, Cho MS, To K (1998) Physica A 254:272–279
7. Gonon P, Foulc JN, Atten P, Boissy C (1999) J Appl Phys 86:7160–7169
8. Conrad H, Wu CW, Tang X (1999) Int J Mod Phys B 13: 1729–1738
9. Hao T (2001) Adv Mater 13:1847–1857
10. Hao T, Xu Z, Xu Y (1997) J Colloid Inter Sci 190:334–340
11. Bossis G, Abbo C, Cutillas S, Lacis S, Métayer C (2001) Int J Mod Phys B 15:564–573
12. Boissy C, Atten P, Foulc JN (1996) J Intell Mater Sys Struct 7:599–603
13. Kim JW, Choi HJ, Lee HG, Choi SB (2001) J Ind Eng Chem 7:218–222

14. Kim SG, Kim JW, Jang WH, Choi HJ, Jhon MS (2001) Polymer 42:5005–5012
15. Sim IS, Kim JW, Choi HJ, Kim CA, Jhon MS (2001) Chem Mater 13:1243–1247
16. Men S, Xu X, Lan Y, Xu S, Lu K (2001) Int J Mod Phys B 15:788–794
17. Trlica J, Saha P, Quadrat O, Stejskal J (2000) J Phys D Appl Phys 33:1773–1780
18. Lee YH, Kim CA, Jang WH, Choi, HJ Jhon MS (2001) Polymer 42:8277–8283
19. Saito T, Anzai H, Kuroda S, Osawa Z(1999) Int J Mod Phys B 13:1689–1696
20. Kim JW, Kim SG, Choi HJ, Jhon MS (1999) Macromol Rapid Commun 20:450–452
21. Kim JW, Kim SG, Choi HJ, Suh MS, Shin MJ, Jhon MS (2001) Int J Mod Phys B 15:657–664
22. Barthet C, Armes SP, Lascelles SF, Luk SY, Stanley HME (1998) Langmuir 14:2032–2041
23. Cairns DB, Armes SP, Bremer LGB (1999) Langmuir 15:8052–8058
24. Khan MA, Armes SP (2000) Adv Mater 12:671
25. Shen S, Sudol ED, El-Aasser MS (1994) J Polym Sci A Polym Chem 32:1087
26. Choi HJ, Kim TW, Cho MS, Kim SG, Jhon MS (1997) Eur Polym J 33:699–703
27. Cho MS, Kim JW, Choi HJ, Webber RM, Jhon MS (2000) Colloid Polym Sci 278:61–64
28. Kim SG, Kim JW, Choi HJ, Suh MS, Shin MJ, Jhon MS (2000) Colloid Polym Sci 278:894–898
29. Choi HJ, Lee JH, Cho MS, Jhon MS (1999) Polym Eng Sci 39:493–499
30. Jang WH, Kim JW, Choi HJ, Jhon MS (2001) Colloid Polym Sci 279:823–827
31. Choi HJ, Cho MS, Kim JW (2001) Korea-Aust Rheol J 13:197–203
32. Cho MS, Choi HJ, Chin IJ, Ahn WS (1999) Micropor Mesopor Mater 32:233–239
33. Shih YH, Conrad H (1994) Int J Mod Phys B 8:2835–2853
34. Choi, HJ, Kim JW, To K (1999) Polymer 40:2163–2166
35. Kim JW, Choi HJ, Jhon MS (2000) Macromol Symp 155:229–237
36. See H, Kawai A, Ikazaki F (2002) Colloid Polym Sci 280: 24–29
37. Lee JH, Cho MS, Choi HJ, Jhon MS (1999) Colloid Polym Sci 277:73–76
38. Hao T (1997) Appl Phys Lett 70:1956–1958
39. Webber RM (1995) In: Havelka KO, Filisko FE (eds) Progress in electrorheology. Plenum, New York, pp 171–184
40. Scaife BKP (1989) Principles of dielectrics. Clarendon, Oxford, pp 66–67